

Solution of a separable Smoluchowski equation in one spatial dimension

I. Klik and Y. D. Yao

Institute of Physics, Academia Sinica, Taipei 115, Taiwan

(Received 2 August 1999; revised manuscript received 20 April 2000)

An approximate solution of a separable Smoluchowski equation in one spatial dimension is constructed here in the form of a finite eigenfunction expansion. The spectrum of the Smoluchowski operator, and the corresponding eigenfunctions, are computed using the so called shooting method of adjoints. Explicit numerical solutions are presented for static and fluctuating potentials, and it is shown that for any smooth initial probability distribution the finite expansion holds on all time scales. The method is applicable to any linear eigenproblem on a finite one-dimensional interval; the solution of the Sturm-Liouville problem has a particularly convenient form.

PACS number(s): 02.60.Lj, 05.40.-a

I. INTRODUCTION

We present here a systematic method of constructing the solution of a separable partial differential equation with arbitrary precision. The proposed formalism is based on the so called shooting method of adjoints [1], which allows the conversion of a linear two-point boundary value problem into an initial value one. The main idea of the method is simple: Let the boundary value problem on $\langle x_1, x_2 \rangle$ be given by the N linear equations

$$y'_i(x) = \sum_{j=1}^N A_{ij}(x)y_j(x) + f_i(x), \quad (1)$$

$y'_i = dy_i/dx$, to be solved subject to N_1 boundary conditions at $x = x_1$ and $N_2 = N - N_1$ boundary conditions at $x = x_2$. Corresponding to Eq. (1) is the adjoint equation

$$\xi'_i(x) = - \sum_{j=1}^N A_{ji}(x)\xi_j(x), \quad (2)$$

and by construction any two solutions $\vec{y}(x)$ and $\vec{\xi}(x)$ of Eqs. (1) and (2) satisfy the identity

$$\vec{y}(x_2) \cdot \vec{\xi}(x_2) - \vec{y}(x_1) \cdot \vec{\xi}(x_1) = \int_{x_1}^{x_2} dx \vec{f}(x) \cdot \vec{\xi}(x). \quad (3)$$

Equation (2) has infinitely many solutions, but with a suitable choice of initial conditions it is always possible to find a set of N linearly independent solutions $\vec{\xi}^{(k)}(x)$, $k = 1, 2, \dots, N$, such that an N -fold application of the identity (3) yields a solvable $N \times N$ linear system for the missing N boundary values at $x = x_1$ and x_2 .

Of particular interest to us here will be the separable Smoluchowski equation [2]

$$\frac{\partial P(x,t)}{\partial t} = \frac{\partial}{\partial x} \left(V'(x) + \frac{\partial}{\partial x} \right) P(x,t) \stackrel{\text{def}}{=} \mathcal{S}_V P(x,t) \quad (4)$$

in which $V' = dV/dx$ is independent of time, and the operator \mathcal{S}_V is defined for future convenience. The formal solution of Eq. (4) is [2]

$$P(x,t) = \sum_{n=0}^{\infty} e^{\lambda_n t} Q_n(x), \quad (5)$$

$$\lambda_n Q_n(x) = \frac{d}{dx} \left(V'(x) + \frac{d}{dx} \right) Q_n(x), \quad (6)$$

but Eq. (4) is usually solved by approximate methods of propagating the initial distribution $P(x,0)$ in time. Thus the implicit marching scheme (see, e.g., Sec. 197 of Ref. [3]) yields excellent results for evolution within a single local minimum of the potential V , but fails (in our experience) if the evolution also involves an overbarrier probability flux. In this case, the first nonzero eigenvalue of Eq. (4) is close to zero, and round-off errors appear to systematically render it (for reasons unclear to us) identically equal to zero, causing the scheme to converge toward an incorrect stationary state. A similar problem with disparate time scales is known also in power series expansions [4] of the propagator $\exp[\mathcal{S}_V t]$. The shooting method of adjoints, by contrast, leads to a finite expansion of the form (5), which is valid, for a smooth initial distribution $P(x,0)$, on all time scales.

II. THE SMOLUCHOWSKI EQUATION

The Smoluchowski equation (4) assumes the form (1) under a Laplace transform,

$$\frac{d}{dx} \begin{pmatrix} \hat{P}' \\ \hat{P} \end{pmatrix} = \begin{pmatrix} -V' & p - V'' \\ 1 & 0 \end{pmatrix} \begin{pmatrix} \hat{P}' \\ \hat{P} \end{pmatrix} - P(x,0) \begin{pmatrix} 1 \\ 0 \end{pmatrix}, \quad (7)$$

with $\hat{P} = \hat{P}(x,p) = \mathcal{L}P(x,t)$ and $\hat{P}' = d\hat{P}/dx$. The corresponding adjoint equation is defined by Eq. (2), and in order to select a suitable solution of this equation we must now impose boundary conditions on the distribution $P(x,t)$. We choose first a symmetric problem with $V(x) = V(-x)$ and $P(x,t) = P(-x,t)$, and with the absorbing boundary conditions $P(\pm 1,t) = 0$. By symmetry there is then also $\hat{P}'(1,p) = -\hat{P}'(-1,p)$, and with the choice $\vec{\xi}(-1,p) = (0,1)$ Eq. (3) finally yields

$$\hat{P}'(-1,p) = \frac{1}{\xi_1(1,p)} \int_{-1}^1 dx P(x,0) \xi_1(x,p), \quad (8)$$

whence

$$\mathcal{L}^{-1} \hat{P}'(-1,p) = \sum_{n=0}^{\infty} e^{\lambda_n t} Q_n'(-1) \quad (9)$$

for the desired values of λ_n and $Q_n'(-1) = -Q_n'(1)$. The poles of $\hat{P}'(-1,p)$ in the complex p plane are defined by the function $\xi_1(x,p)$ which, according to Eqs. (2) and (7), satisfies the Volterra integral equation

$$\begin{aligned} \xi_1(x,p) = & -e^{-V(-1)} \int_{-1}^x du e^{V(u)} + p \\ & \times \int_{-1}^x du_1 e^{V(u_1)} \int_{-1}^{u_1} du_2 \xi_1(u_2,p) e^{-V(u_2)}, \end{aligned} \quad (10)$$

which is easily solved using the method of Piccard iterations (see, e.g., Sec. 145 of Ref. [3] and Refs. [5,6]). For regular potentials V the function $\xi_1(x,p)$ is free of poles, and the function $\xi_1(1,p)$ has infinitely many zeros along the negative real axis of the complex p plane. These zeros, $\xi_1(1,\lambda_n) = 0$, represent the eigenvalues λ_n , and the derivatives $Q_n'(-1)$ then follow from the key relation

$$Q_n'(-1) \frac{d\xi_1(1,\lambda_n)}{dp} = \int_{-1}^{-1} dx P(x,0) \xi_1(x,\lambda_n). \quad (11)$$

In solving Eq. (10) we use the known exact solution $\xi_1(x,0)$ as an initial estimate for iterations of $\xi_1(x,-dp)$, and then repeat the procedure until a sufficiently large p interval is covered. The high order zeros of $\xi_1(x,p)$, moreover, are almost equidistant on the scaled axis $p = -r^2$, and the bracketing of λ_n may thus be speeded up if in place of the decrements $-dp$ one uses the increments dr . In this manner we found it easy to bracket all eigenvalues $\lambda_n \in \langle -10^4, 0 \rangle$. The derivatives $d\xi_1(1,\lambda_n)/dp$ may be obtained by interpolation, or, alternatively, by formally differentiating Eq. (10) with respect to p and solving the resultant integral equation for $\partial \xi_1(x,\lambda_n)/\partial p$.

With the values λ_n , $Q_n(-1)$, and $Q_n'(-1)$ known, we rewrite Eq. (6) as an integral equation and solve it iteratively [7]. We recall that the derivatives $Q_n'(-1)$ defined by Eq. (11) are specific to a given initial distribution, but the problem is linear, and it is therefore possible to solve Eq. (6) with $Q_n'(-1) = 1$ and then to set $Q_n(x) \rightarrow Q_n'(-1) Q_n(x)$, where $Q_n'(-1)$ are the computed boundary values.

III. THE PROBABILITY DISTRIBUTION

Here we present some examples of computed distributions $P(x,t)$. Absorbing boundary conditions are assumed, and the barrier heights are chosen so as to yield wide, easily plotted functions.

As a first example we present in Fig. 1 symmetric solutions of Eq. (4) for the monostable potential $V(x) = 10 \sin^2(\pi x/2)$ on $\langle -1, 1 \rangle$. The long-time decay of this sys-

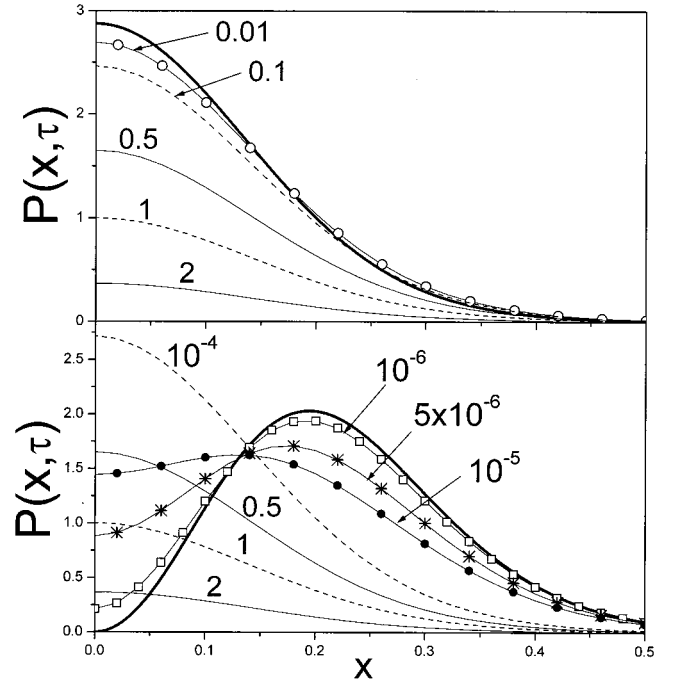


FIG. 1. The probability distribution $P(x,\tau) = P(-x,\tau)$ versus x at selected reduced times τ as labeled. The potential $V(x) = 10 \sin^2(\pi x/2)$, and the points $x = \pm 1$ are absorbing. The one- and two-peaked (see text) initial distributions $P_1(x,0)$ (top) and $P_2(x,0)$ (bottom) are shown in heavy lines.

tem is governed by the first eigenvalue $\lambda_1 \approx -1.35 \times 10^{-3}$ and by the corresponding eigenfunction $Q_1(x) = Q_1(-x)$. The contributions of $Q_2(x) = -Q_2(-x)$, with $\lambda_2 \approx -66.2$, and of $Q_{2n}(x)$, $n=2,3,\dots$, vanish by symmetry. We consider here the two normalized initial distributions

$$P_1(x,0) = \mathcal{N}_1 (1-x^2) e^{-V(x)},$$

$$P_2(x,0) = \mathcal{N}_2 x^2 (1-x^2) e^{-V(x)},$$

which have a single and a double maximum on $\langle -1, 1 \rangle$, respectively. The distribution $P_1(x,0) \approx Q_1(x)$, so that it is close to the quasistationary state postulated for a metastable state by Kramers [8]. Indeed, on the time scale $\tau = -\lambda_1 t$ this distribution undergoes almost no evolution at all for $\tau \lesssim 10^{-3}$, while at later times it decays exponentially. $P_2(x,0)$, on the other hand, evolves initially rapidly toward the Kramers quasistationary state, and then decays exponentially as well.

Our second example is the bistable potential $V(x) = 5 \cos^2(\pi x)$ on $\langle -1, 1 \rangle$. The first two eigenvalues in this case approach degeneracy, with $\lambda_1 \approx -0.186$ and $\lambda_2 \approx -0.377$ corresponding to an even and an odd eigenfunction, respectively. We consider here a double peaked initial distribution centered in the right hand well; the problem is thus asymmetric, and requires two solutions of the adjoint Eq. (2), with $\tilde{\xi}^{(1)}(-1,p) = (0,1)$ and $\tilde{\xi}^{(2)}(-1,p) = (1,0)$. According to Fig. 2 the evolution again has a transient initial stage of rapid local equilibration followed by a period of Markovian overbarrier decay, with the left well population totally independent of the detailed form of the initial distribution

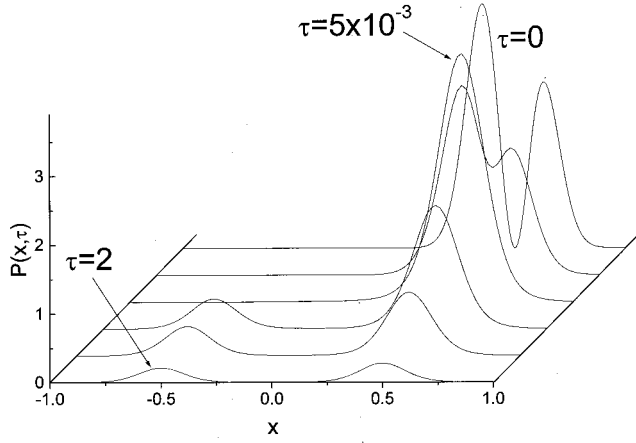


FIG. 2. The asymmetric probability distribution $P(x, \tau)$ versus x at selected reduced times $\tau=0$ (labeled), 5×10^4 , 5×10^{-3} (labeled), 5×10^{-1} , 1, and 2 (labeled). The potential $V(x) = 5 \cos^2(\pi x)$, and the points $x = \pm 1$ are absorbing. The initial distribution $P(x, 0) = \mathcal{N}(\bar{x}, \omega^2)$ where $\bar{x} = x - 1/2$ and $\omega = 5\pi^2$.

within the right well. Interestingly, Fig. 2 also shows that the left well population forms a persistent quasistationary state.

In Fig. 3, finally, we present the case of a three-step cascade given by the potential $V(x) = \cos^2(\pi x/2) - x$ with absorbing boundaries at $x_1 = -2 - x'$ and $x_2 = 4 - x'$, where $\pi x' = \arctan 2(\pi^2 - 4)^{-1/2}$. This system is distinguished by its dense spectrum: The functions $\hat{P}'(x_i, p)$ here have over 1700 poles on the p interval $(-10^4, 0)$, as compared to only about 65 poles in the two cases above.

In all cases we find that the numerical result at $t=0$ represents the prescribed smooth initial distribution $P(x, 0)$ to an excellent degree of accuracy, and we therefore conclude that our finite approximation is valid on both the intrawell and the overbarrier time scales.

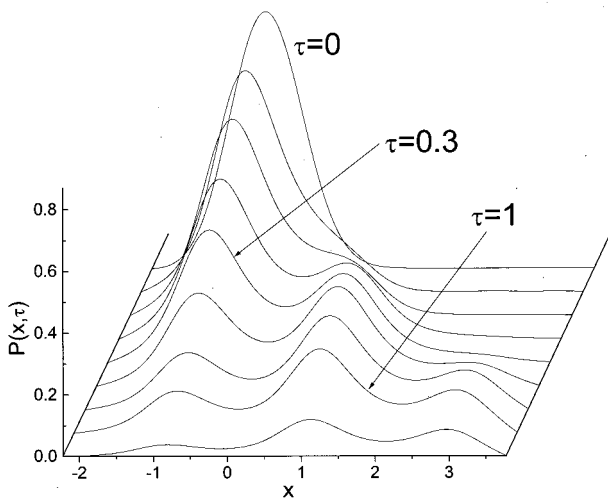


FIG. 3. The probability distribution $P(x, \tau)$ versus x at selected reduced times $\tau=0$ (labeled), 5×10^{-2} , 1×10^{-1} , 2×10^{-1} , 3×10^{-1} (labeled), 5×10^{-1} , 8×10^{-1} , 1 (labeled), and 2. The potential $V(x) = \cos^2(\pi x/2) - x$, and the points $x_1 = -2 - x'$ and $x_2 = 4 - x'$, $\pi x' = \arctan 2(\pi^2 - 4)^{-1/2}$, are absorbing. The initial distribution $P(x, 0) = \mathcal{N}(x - x_1)(x - x_2) \exp(-\omega x^2)$ where $\bar{x} = x - x_m$, $x_m = -1 + x'$, and $\omega = -(\pi/2)^2 \cos(\pi x_m)$.

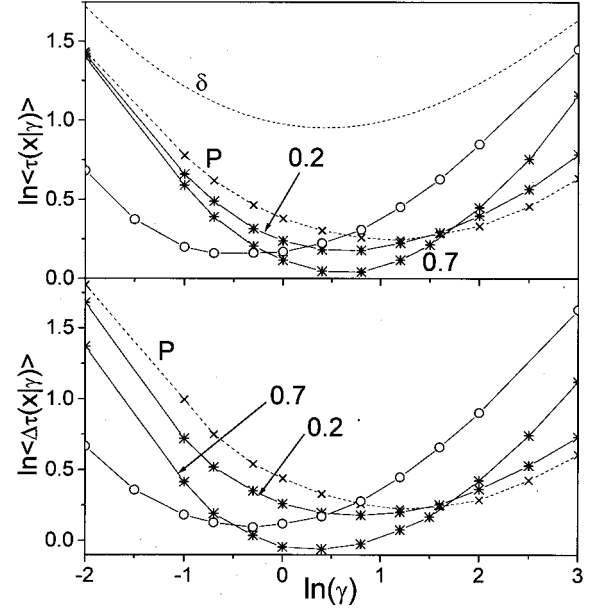


FIG. 4. Top: The mean first passage time $\langle \tau(x|\gamma) \rangle$ versus the inverse mean waiting time γ . Dashed lines represent results for Markovian and solid lines for non-Markovian flip events. The dashed line labeled δ was calculated according to Ref. [6], and the dashed line labeled P is the result of numerical simulations based on Eq. (13). \star -marked solid lines represent simulations based on Eq. (15), with ρ values as labeled, and the \circ -marked solid curve is based on the distribution (16). Bottom: The mean square deviation $\langle \Delta \tau(x|\gamma) \rangle^2$ versus the inverse mean waiting time γ . Markings and labels as above; the $P(x, 0) = \delta(x)$ result is not known to us.

IV. A FLUCTUATING BARRIER

Systems that exhibit dichotomic Markovian fluctuations are described by the equation [9]

$$\frac{\partial}{\partial t} \begin{pmatrix} P_1 \\ P_2 \end{pmatrix} = \begin{pmatrix} \mathcal{S}_{V_1} - \gamma & \gamma \\ \gamma & \mathcal{S}_{V_2} - \gamma \end{pmatrix} \begin{pmatrix} P_1 \\ P_2 \end{pmatrix}, \quad (12)$$

where the operators \mathcal{S}_{V_i} have been defined by Eq. (4). The potential here switches randomly between the values $V_1(x)$ and $V_2(x)$, and the waiting times between individual flips have the exponential distribution

$$D(t) = \gamma e^{-\gamma t} \quad (13)$$

and the expectation value $\langle t \rangle = \gamma^{-1}$. The separable Eq. (12) is amenable to direct treatment by the shooting method, but its eigenvalues are complex [10], and locating them may be too demanding. We therefore propose to solve Eq. (12) by means of a numerical simulation in which we generate [11] a series of random waiting times t_1, t_2, t_3, \dots with the distribution (13), and then use the known propagators $\exp[\mathcal{S}_{V_i} t]$ to successively calculate the probability distribution on the intervals $\langle 0, t_1 \rangle, \langle t_1, t_1 + t_2 \rangle, \dots$. At $t=0$ the potential V is with equal probability in the state V_1 or V_2 .

We assume absorbing boundaries at $x_i = \pm 1$, symmetric potentials $V_1(x) = 10x^2$ and $V_2(x) \equiv 0$, and a smooth initial distribution $P(x, 0) = \mathcal{N}(1 - x^2) e^{-V_1(x)}$. The quantities of interest are the moments of the mean first passage time

$$\langle \tau^n(x|\gamma) \rangle = n \int_0^\infty dt t^{n-1} \int_{-1}^1 d\bar{x} [P_1(\bar{x}, t) + P_2(\bar{x}, t)] \quad (14)$$

averaged over the initial position of the particle.

The computed first moment $\langle \tau(x|\gamma) \rangle$ is compared with the function $\tau(0|\gamma)$ calculated according to Ref. [6] in Fig. 4. There is, obviously, $\langle \tau(x|\gamma) \rangle < \tau(0|\gamma)$ for all rates γ , and the local minimum of $\langle \tau(x|\gamma) \rangle$ shifts to higher flip rates due to the decreased effective barrier height [6].

In the Markovian distribution (13) the most probable waiting time is zero. However, cases where an immediate jump occurs with zero probability arise quite naturally in the context of exit out of a metastable domain (see Sec. IV and Ref. [5]), and we approximate them by introducing the cutoff time t_s ,

$$D(t) = \begin{cases} 0 & \text{if } t < t_s \\ \kappa e^{-\kappa(t-t_s)} & \text{if } t > t_s, \end{cases} \quad (15)$$

and the normalization $\langle t \rangle = \gamma^{-1}$. In parametric form there is then $t_s = \rho \gamma^{-1}$ and $\kappa = \gamma(1-\rho)^{-1}$, and Eq. (15) goes over to the Markovian limit (13) as $\rho \rightarrow 0$. Figure 4 shows that the mean first passage time computed according to Eq. (15) exhibits stronger resonance at lower inverse mean waiting times γ than in the case of Markovian flips. At large $\rho \rightarrow 1$ the rate κ tends to infinity, and the distribution (15) becomes very sharp, suppressing both short- and long-duration flips. In order to isolate this effect we introduce also the distribu-

$$D(t) = \frac{1}{1 - e^{-\kappa t_s}} \begin{cases} \kappa e^{-\kappa t} & \text{if } t < t_s \\ 0 & \text{if } t > t_s \end{cases} \quad (16)$$

with the normalization $\langle t \rangle = \gamma^{-1}$ and parametrization $t_s = \rho \gamma^{-1}$. Curiously, the resultant mean first passage time $\langle \tau(x|\gamma) \rangle$ again exhibits enhanced resonance at lower flip rates (inverse mean waiting times, see Fig. 4), and we therefore propose (with no strict proof) that the Markovian distribution of waiting times leads to the smallest resonance at the highest flip rates. According to Fig. 4, further, the mean square deviation

$$\langle \Delta \tau(x|\gamma) \rangle^2 = \langle \tau^2(x|\gamma) \rangle - \langle \tau(x|\gamma) \rangle^2 \quad (17)$$

is proportional to $\langle \tau(x|\gamma) \rangle^2$, but for the distributions (13) and (15) the ratio $\langle \Delta \tau \rangle / \langle \tau \rangle$ decreases with increasing γ , so that the large-flip-rate exit events are in fact the least noisy. This trend is reversed for the distribution (16) where the ratio $\langle \Delta \tau \rangle / \langle \tau \rangle$ increases with increasing γ .

The above examples demonstrate the utility of the shooting method of adjoints. In conclusion we wish to remark that the method is applicable also to the eigenproblem $\lambda_n Q_n = \mathcal{O} Q_n$ where \mathcal{O} is a linear differential operator in one dimension: The identity (3) is in this case obviously of little help (it leads back to an eigenproblem), but comparing Eqs. (4) and (6) we see that the eigenproblem can be embedded in the parabolic partial differential equation $\partial Q / \partial t = \mathcal{O} Q$, and then solved by the methods of Sec. II. Moreover, if the operator \mathcal{O} is self-adjoint then the computed eigenfunctions are mutually orthogonal, and the embedding yields a solution to the Sturm-Liouville problem on a finite interval.

-
- [1] S. M. Roberts and J. S. Shipman, *Two-Point Boundary Value Problems: Shooting Methods* (American Elsevier, New York, 1972), Chap. 3.
- [2] C. W. Gardiner, *Handbook of Stochastic Methods*, 2nd ed. (Springer-Verlag, Berlin, 1985), Chap. 5.2.
- [3] D. Zwillinger, *Handbook of Differential Equations*, 3rd ed. (Academic Press, San Diego, 1997).
- [4] A.N. Drozdov and S. Hayashi, *J. Chem. Phys.* **110**, 1888 (1999).
- [5] I. Klik and Y.D. Yao, *Phys. Rev. E* **59**, 6444 (1999).
- [6] I. Klik and Y.D. Yao, *Phys. Rev. E* **57**, 6180 (1998).
- [7] S.V.G. Menon, *J. Stat. Phys.* **66**, 1675 (1992); I. Klik and Y.D. Yao, *Phys. Rev. E* **52**, 6892 (1995).
- [8] H.A. Kramers, *Physica* (Amsterdam) **7**, 284 (1940).
- [9] M. Bier and R.D. Astumian, *Phys. Rev. Lett.* **71**, 1649 (1993).
- [10] I. Klik and Y.D. Yao (unpublished).
- [11] I. Klik and Y.D. Yao, *IEEE Trans. Magn.* **34**, 1285 (1998).